

Femtosecond Ionization Source for Ultrahigh Resolution Time-of-flight Mass Spectrometry

W. Ronny Huang, Xiang Li, Anthony W. Yu, William A. Brinckerhoff, Molly Fahey
NASA Goddard Space Flight Center
8800 Greenbelt Rd.
Greenbelt, MD 20771
301-614-6016

w.ronny.huang@gmail.com, xiang.li@nasa.gov, anthony.yu@nasa.gov,
william.brinckerhoff@nasa.gov, molly.fahey@nasa.gov

Abstract—High resolution time-of-flight mass spectrometers (TOFMSs) have broad potential application in space exploration. We propose a novel femtosecond electron ionization (EI) source which, when coupled to a compact TOFMS, could improve mass resolution of miniature instruments by orders of magnitude, enabling effective isobar identification in volatile and planetary atmospheres. The ionization source is an ultrashort pulsed electron gun triggered by a femtosecond UV laser. In addition, the ultrafast laser technology may also be used for other analytical capabilities like laser desorption/ionization on solid samples, therefore future developments may offer a novel compact instrument package for both atmosphere and surface analysis. Here, we show a series of advances toward this goal, including efficient (5%) generation of 105 fs UV pulses, production of electron bunches of up to 32 fC pC via UV photoemission, and calculations for an ultrafast EI source.

TABLE OF CONTENTS

1. INTRODUCTION.....	1
2. FEMTOSECOND TOFMS CONCEPT.....	1
3. PULSED UV LASER SOURCE	2
4. ULTRAFAST, HIGH YIELD ELECTRON GUN	4
5. FUTURE TOFMS INTEGRATION	6
6. CONCLUSION.....	6
ACKNOWLEDGEMENTS.....	6
REFERENCES	7
BIOGRAPHY	8

1. INTRODUCTION

High resolution time-of-flight mass spectrometers (TOFMSs) have broad potential application in planetary exploration, such as rapid isobar identification and detailed isotopic measurements of volatile species, which provide better understanding of the origin and processing of light elements (C, H, O, N, and S), the noble gases, and prebiotic/biogenic organic compounds. For example, to mass-separate formaldehyde (H₂CO, 30.0106 Da) and ethane (C₂H₆, 30.0470 Da), a mass resolution of $m/\Delta m > 824$ is needed [1]. Indeed, the 2013 NASA Decadal Survey lists mass spectrometers on 7 of the 13 priority planetary missions and emblemizes them as a Recommended Technology Investment (“Mass spectrometers [...] would benefit significantly from a science instrument technology program aimed at improving basic instrument performance characteristics.”) [2]. TOFMSs could utilize various

ionization sources to produce ions or fragments from neutral parent molecules. However, it is challenging to achieve ultrahigh mass resolution in the TOFMSs without increasing the size and complexity of the instrument. For example, pulsed laser desorption/ionization (LDI), effectively used for solid sample analysis with mass resolution up to several hundred Da, is typically limited by the few-nanosecond laser pulse duration (Δt). Filament-based electron guns have long been coupled to quadrupole and ion trap mass spectrometers for gas sample analysis via electron impact (EI) ionization, but less commonly to TOFMS since such guns are limited to producing μ s to ms duration ion pulses. To address this challenge, an ultrafast, high density EI source has the potential to produce *picosecond (ps)* or *femtosecond (fs)* ion pulses from gas samples, which will not only improve mass resolution of TOFMSs by 10-100x, but also reduce analysis times through enhanced ionization yield. Here we discuss a series of advances toward an ultrafast laser-triggered EI source, including demonstration of a UV source, demonstration of UV photoemission on copper, design of an ultrafast electron gun, and calculations of the expected ion yield. Further, the ultrafast laser used to trigger the EI source could potentially also be used for LDI in the same instrument package, enabling the possibility of performing both gas analysis and solid sample analysis in a single compact instrument.

2. FEMTOSECOND TOFMS CONCEPT

The fs-TOFMS instrument obtains high mass resolution by reducing the duration, Δt , over which the analyte gas is ionized while also increasing the yield. To achieve a femtosecond ionization EI source, we will leverage two recent technologies typically employed in the particle accelerator community for spaceflight: (1) Ultrafast electron guns delivering high charge density pulsed electron beams and (2) miniature femtosecond UV lasers.

The fs-TOFMS consists of three components:

1. *Laser* – A compact breadboard-based ultrafast laser source producing UV pulses to phototrig the electron gun.
2. *Electron gun (e-gun)* – A miniature, custom-designed electron gun producing ultrashort electron bunches via UV photoelectric emission, accelerating those bunches to the ionization energy (typically 70 eV), and focusing them onto the analyte gas.

3. *TOFMS flight tube and sample chamber* – A TOFMS with sample chamber and flight tube that is integrated with the ultrafast EI source (laser and e-gun) facilitating femtosecond ionization of the analyte gas. The flight tube

analyzes the mass spectra of the gas. Detailed discussion of this component is outside the scope of this paper, which focuses on the EI source.

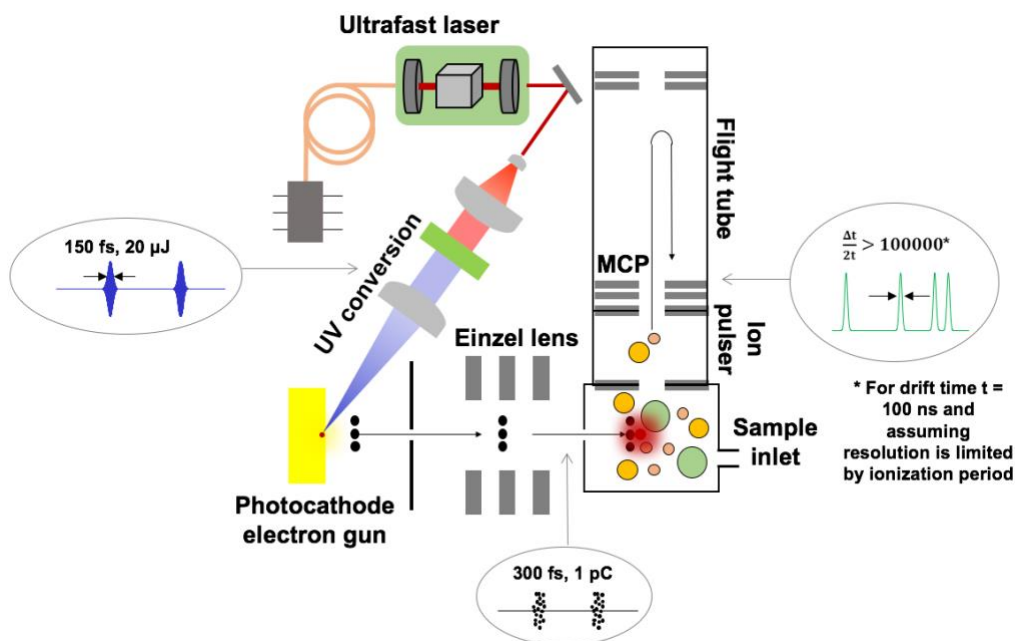


Figure 1. Femtosecond time-of-flight mass spectrometer (fs-TOFMS) concept drawing

An illustration of the complete fs-TOFMS system is shown in Figure 1. The target requirements of our first prototype are shown in Table 1. In Section 3, we present our results of UV pulse generation from two separate pump lasers, In Section 4, we show developments in the electron beam generation, acceleration, focusing, and characterization. In Section 5, we discuss plans to integrate the laser-triggered electron gun with an existing TOFMS sample chamber. We provide concluding remarks in Section 6.

Table 1: Performance targets

UV laser	Wavelength	266 nm or 258 nm
	Pulse duration	<1 ps
	Pulse energy	>5 μJ
	Rep. rate	>1 kHz
Electron gun	Energy	70 eV
	Bunch charge	>1 pC
	Bunch duration	<1 ns
	Spot size on sample	<100 μm
TOFMS	Mass range	<200 Da
	Mass resolution	>1000

3. PULSED UV LASER SOURCE

Photons with energy greater than the workfunction of the ionization surface material are needed to ionize electrons via single-photon photoelectric emission. Although multiphoton

emission is possible, this process is less efficient, requiring large pulse energies which may optically damage the surface. Since the photoelectric workfunction of most metals is 4 eV or larger, photon energies in the UV spectral range (energy calculated by $E = h\nu$) are required for single-photon emission. The duration of the emitted electron bunch is typically longer than the duration of the UV pulse by a few femtoseconds for metals and a few picoseconds for dielectrics due to scattering processes. Thus, short UV pulse durations are needed to yield short electron bunches.

Coherent (laser-like) UV radiation is not available by directly pumping optical materials the way that, i.e., IR radiation is and must be generated by nonlinear upconversion of an IR pump pulse. We tested IR to UV conversion from two pump laser technologies operating at common IR wavelengths: 800 nm and 1030 nm. Since the pump laser determines downstream parameters and consumes a large fraction of the power of the system, we took care to characterize their performances and compare their merits. A summary is provided in Table 2. The two major technologies are discussed next.

UV generation pumped by 800 nm Ti:Sapphire laser

Ti:Sapphire lasers have one of the largest gain bandwidths of any laser material and, via Kerr-lens modelocking, routinely outputs pulses as low as 10 fs in laboratory settings. The downside of such lasers, however, is that they produce a lot of excess energy given their quantum defect of 38%. Further,

their modelocking requires extremely stable situations, which are not possible in spaceflight. Miniature, monolithic Ti:Sapphire systems capable of spaceflight have been built [3] albeit with Q-switching instead of modelocking at 700 ps duration.

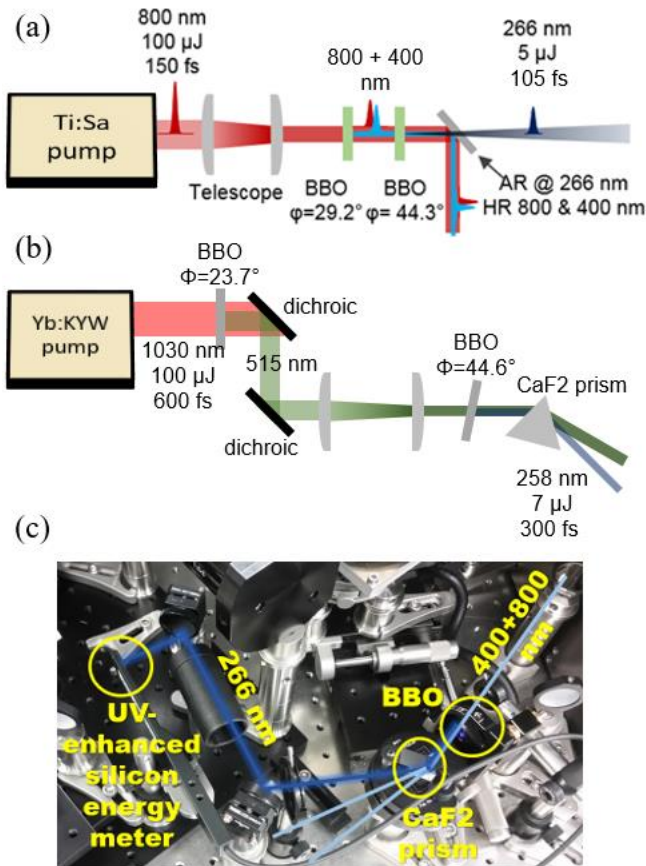


Figure 2. Schematic of the UV generation setup using a (a) 800 nm Ti:Sapphire (Ti:Sa) pump and (b) 1030 nm Yb:KYW pump. (c) Photograph of the 800 nm pump setup from (a). Note that the CaF₂ prism was eventually replaced with several dichroics to separate out the UV beam.

Femtosecond UV pulses with wavelength $\lambda=266$ nm were obtained in the lab by third harmonic generation of a 800 nm Ti:Sapphire pump laser (Coherent) with pulse duration of 150 fs and 100 μ J of energy (schematic and photograph shown in Figure 2(a) and 2(c)). The first conversion stage consisted of a 0.1 mm thick, type-I BBO crystal (Cstech) with c-axis angled at $\phi=29.2^\circ$ to facilitate efficient phase-matched generation of 400 nm pulses. The 800 and 400 nm pulses then propagate together (with temporal walkoff of approximately 60 fs) toward the second conversion stage consisting of a 0.5 mm type-I BBO angled at $\phi=44.3^\circ$, which is phase-matched for sum frequency mixing of the 800 and 400 nm light to produce 266 nm light. Three dichroic beamsplitters (LayerTec) were used to isolate the 266 nm UV beam from the 800 nm and 400 nm beams.

The total conversion efficiency achieved was around 5%, yielding 5 μ J UV pulses. Figure 3(a) and (b) show the optical spectra of the 800 and 400 nm pulses, respectively. Since both nonlinear conversions were operated in the unsaturated regime and the phase-matching bandwidths of both BBO crystals are broader than the spectral bandwidths of both the 800 nm and 400 nm pulses, we expect the UV pulsewidth to be roughly $1/\sqrt{3}$ that of the pump laser, or 87 fs. Based on a Fourier transform of the measured spectra of the UV pulse (Figure 3(c)), which has a bandwidth of 1.05 nm, and assuming the pulse is transform-limited, the pulse duration is 105 fs.

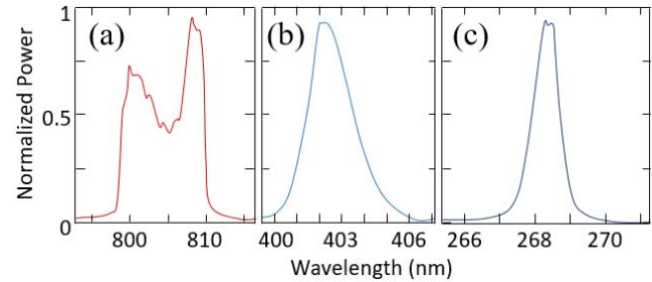


Figure 3. Measured optical spectra of the (a) 800 nm pump, (b) 400 nm second harmonic, and (c) 266 nm UV from sum frequency generation of the 800 and 400 nm beams.

UV generation pumped by 1030 nm Yb-doped laser

Pulsed Yb-doped lasers have been extensively manifested in fibers, microchips, or free space cavities, all of which have common properties of ~ 1 μ m center wavelength and low heat generation due to small quantum defect (8%). A downside of Yb-doped lasers is that their typical output bandwidth is not as wide as that of the Ti:Sapphire laser; thus their pulse durations go down to 100 fs at best and a few hundred ps typically. This not only reduces the nonlinear conversion efficiency but also it limits the resolution enhancement that can be achieved in TOFMS.

UV pulses at 258 nm were generated in the lab by frequency-quadrupling 1030 nm, 600 fs pulses from a Yb:KYW regenerative amplifier with 100 μ J of energy. The first second-harmonic generation (SHG) stage consisted of a 0.5 mm thick type I BBO crystal with $\phi=23.7^\circ$, generating approximately 3 μ J of 515 nm pulses. The second SHG stage consisted of 0.5 mm thick type I BBO crystal cut for $\phi=44.6^\circ$ but tilted to $\sim 50^\circ$, generating 600 nJ of 258 nm pulses. The conversion efficiency from 1030 nm to 258 nm was about 7%, yielding 7 μ J of UV energy. The reason that this conversion efficiency is higher than that of the first experiment with Ti:Sapphire pump, even though the Ti:Sapphire had shorter pulses, is because of the temporal walkoff between the 800 and 400 nm pulses in the first

Table 2: Pump laser architectures/parameters

Modelocked pump		Microchip pump
Ti:Sapphire	Yb:KYW	Yb:YAG
$\tau_{\text{available}} = 150 \text{ fs}$	$\tau_{\text{available}} = 600 \text{ fs}$	$\tau_{\text{available}} = 800 \text{ ps}$
$\tau_{\text{min}} = 10 \text{ fs}$	$\tau_{\text{min}} = 200 \text{ fs}$	$\tau_{\text{min}} = 50 \text{ ps}$
Energy = 100 μJ	Energy = 100 μJ	Energy = 100 μJ
$\lambda = 800 \text{ nm}$	$\lambda = 1030 \text{ nm}$	$\lambda = 1030 \text{ nm}$
$\lambda_{\text{UV}} = 266 \text{ nm}$	$\lambda_{\text{UV}} = 258 \text{ nm}$	$\lambda_{\text{UV}} = 258 \text{ nm}$
Rep. rate = 1 kHz	Rep. rate = 1 kHz	Rep. rate = 2-11 kHz
Wallplug $\sim 1\%$	Wallplug $> 10\%$	Wallplug $> 10\%$
Lifetime* $> 1\text{B}$	Lifetime $> 1\text{B}$	Lifetime $> 1\text{B}$
Vol. $\sim 10000 \text{ cm}^3$	Vol. $\sim 10000 \text{ cm}^3$	Vol. $\sim 50 \text{ cm}^3$

τ_{min} – minimum achievable pulsewidth from literature

$\tau_{\text{available}}$ – current available pulsewidth for test

* in units of laser pulses (shots)

experiment. A CaF_2 prism was used to spatially separate the various wavelengths. The prism-induced angular dispersion over the subsequent 0.5 m propagation was determined through calculations to cause negligible increase of the pulse duration. Again, both nonlinear conversions were in the unsaturated regime and the phase-matching bandwidths of the two BBO crystals are broader than the spectral bandwidths of both the 1030 nm and 515 nm pulses, so therefore, we estimate of the UV pulse duration as roughly half that of the fundamental, or about 300 fs.

To achieve the desired pump laser parameters in a compact, robust package, we are preparing to perform UV generation on a Q-switched 1030 nm microchip laser with pulse duration in the 800 ps range. Testing an additional laser architecture (microchip vs. free space cavity) enables us to evaluate the trade-off between improved resolution (shorter pulse duration from free space) on one hand and compact instrument size (microchip is smaller) on the other. Table 2 lists the parameters for both pulsing mechanisms.

Radiation hardening

There have been a number of studies regarding radiation hardening of pump diodes [4,5] showing promising results. Pumps at 980 nm have been used on the LLC (qualified by MIT/LL) and LCRD (qualified by NASA GSFC) missions. Such pumps are similar to those used to pump Yb:YAG microchip lasers, which are typically pumped at 940 nm but can also be pumped at 980 nm. As for Ti:Sapphire pumping at 532 nm, doubled Nd:YAG lasers operating in that wavelength have been flown on multiple spaceflight missions, such as ICESat I/GLAS, CALIPSO, and CATS. BBO nonlinear crystals have also been shown to exhibit negligible degradation from irradiation tests in [6].

DUV solarization

According to a study by ESA on using various nonlinear crystals for space [7], there was no decrease in DUV third-harmonic conversion efficiency over 60 million shots. In fact, the Mars MOMA mission is also using a BBO crystal operating at 266 μm [6]. Due to the high temperature sensitivity of the BBO crystal, the crystal head must be attached to a temperature-controlled heater, as in [6]. To minimize DUV solarization of the BBO crystal, one could operate it at elevated temperature for thermal bleaching, which has proven to be effective in minimizing darkening due to solarization.

Power consumption and lifetime

The demonstrated wall-plug efficiency of our current microchip laser is 12% while the wall-plug efficiency of Ti:Sapphire lasers are on the order of a percent. Lifetime of the lasers can be extended by having redundant pump diodes running at significant derating with their power combined.

4. ULTRAFAST, HIGH YIELD ELECTRON GUN

A laser-triggered electron gun will be developed to generate an electron beam with picosecond or femtosecond duration. The ultrafast UV laser described in Section 3 ionizes a short electron bunch inside the gun via photoelectric *emission* on a photocathode. The liberated electron bunch is then *accelerated* by a static electric field produced inside the gun by applying voltages on metal electrodes. As the bunch propagates, it spreads due to Coulomb repulsion between the individual electrons (henceforth called space charge forces) as well as to the spread in their initial velocity. Consequently, the bunch is then *focused* onto the analyte chamber some distance from the gun using an electrostatic lens. Finally, the electron bunch at the focus point is *characterized* to for live-alignment of the gun and for determining its performance. Figure 4 illustrates these four stages: emission, acceleration, focusing, and characterization.

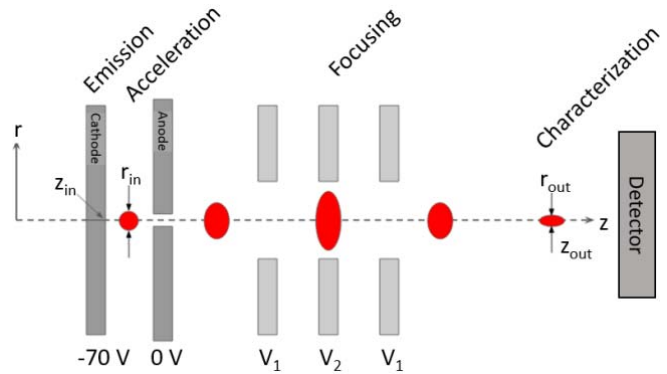


Figure 4. Cross-sectional schematic of the electron gun as well as the electron bunch (red) at various points of propagation.

Table 3: Photocathode materials

Copper	Cesium Telluride	Cesium dispenser
QE: 10^{-6} - 10^{-5}	QE: 10^{-3} - 10^{-2}	QE: 10^{-3} - 10^{-2}
$P < 10^{-5}$ Torr	$P < 10^{-9}$ Torr	$P < 10^{-9}$ Torr
$\Phi_w = 4.6$ eV	$\Phi_w \sim 2.6$ eV	$\Phi_w \sim 2.6$ eV
Very robust	Volatile	Requires apparatus for improved robustness

Φ_w : Work function

QE: Quantum efficiency

Emission

As discussed in Section 3, electrons are produced via UV photoemission on a photocathode substrate. Various photocathodes are being considered for the EI source. Conventional metal (i.e. copper) cathodes are robust and have tolerant vacuum requirements, whereas Cesium based photocathodes have orders of magnitude higher quantum efficiency but also stringent vacuum requirements, which, if violated, will result in failure of the material to further emit electrons. Cesium based cathodes tend to also degrade over time due to the strong electropositivity of Cesium. A 10x improvement in lifetime has been achieved using a Cesium dispenser photocathode in which the layer of Cesium is rejuvenated via heating a Cs:Bi reservoir [8]. Table 3 summarizes the photocathodes under consideration.

We have performed an initial UV photoemission demonstration on a copper substrate, shown in Figure 5. As expected, the charge increases linearly with the UV emitter energy, indicating single-photon emission. The quantum efficiency measured from this data is 5.8×10^{-7} .

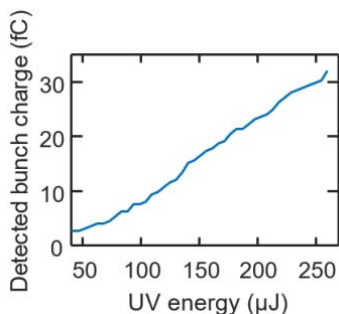


Figure 5. Measured electron bunch charge as a function of the UV photoemitter energy.

Acceleration

EI sources accelerate electrons to the standard energy of 70 eV to facilitate optimal ionization efficiency, since at 70 eV the de Broglie wavelength of the electrons matches the length of typical bonds in organic molecules (0.14 nm). A bias of -70 V is applied on the photocathode to cause the UV-emitted electrons to be repelled (i.e. accelerated) toward the grounded anode where they escape the acceleration region through an iris aperture. Given a vacuum field breakdown threshold of 10 MV/m [9], the cathode-anode gap length can be as compact as 7 μm.

Focusing

The electron bunch spreads transversely immediately after emission due to the spread in transverse velocity as well as to space charge forces. Thus it is important to refocus the bunch onto the sample analyte gas to achieve maximum ionization. We will use an electrostatic (Einzel) lens consisting of a series of three apertures biased at V_1 , V_2 , and V_1 , respectively (see Figure 4) to refocus our electron bunch with a focal length of

$$f = \left[\frac{-3}{8dR} (1 - R^2)(R - 1)(3 - R) \right]^{-1}$$

where $R = \sqrt{V_2/V_1}$ and d is the spacing between the apertures. For a reasonably compact focal length of 1 cm, our parameters are $d=6.3$ mm and $R=2.3$.

End-to-end simulations of the acceleration and focusing of the electron bunch will be pursued in COMSOL to understand the behavior of the electron gun. Thus far, we have simulated the field distribution around the iris apertures in the anode (Figure 6(a)-(b)) and in the electrostatic lens and validated them using the analytical solution (Figure 6(c)). Assembling these aperture unit modules into the full system shown in Figure 6, and then performing particle tracing simulations, will allow accurate predictions of the electron bunch propagation behavior.

Characterization

The electron beam at the focus can be characterized in charge, energy, spatial profile and temporal profile. Absolute charge can be characterized via a Faraday cup connected to a sensitive ammeter, while the energy spectrum of the bunch can be characterized via a homemade retarding field spectrometer as described in the supplementary materials section of [10]. Absolute charge would give an estimate of the eventual ionization yield (see calculations in Section 5), while narrow energy spectra centered at 70 eV would ensure that the bunch is temporally short.

The spatial profile can be obtained by placing a multi-channel plate (MCP) and phosphor screen combination at the focus of the bunch and imaging the light from the phosphor screen using a sensitive camera. Live characterization of the focus spot is critical to aligning the electrostatic lens voltages to ensure that the beam focuses where it should.

The temporal profile can be obtained directly using a fast MCP (Ultrafast Gen2 by Photonic Inc.) which has a response time of 120 ps. This MCP can give a direct measure of the pulse shape (for $\tau_{\text{bunch}} > 120$ ps) or an upper bound on the electron pulse duration (for $\tau_{\text{bunch}} < 120$ ps).

For pulse durations shorter than 120 ps, temporal profile characterization can be achieved via streaking methods [11], but such methods are laborious and complicated. Instead, we could indirectly infer the temporal duration using the electron energy spread from the measured energy spectrum.

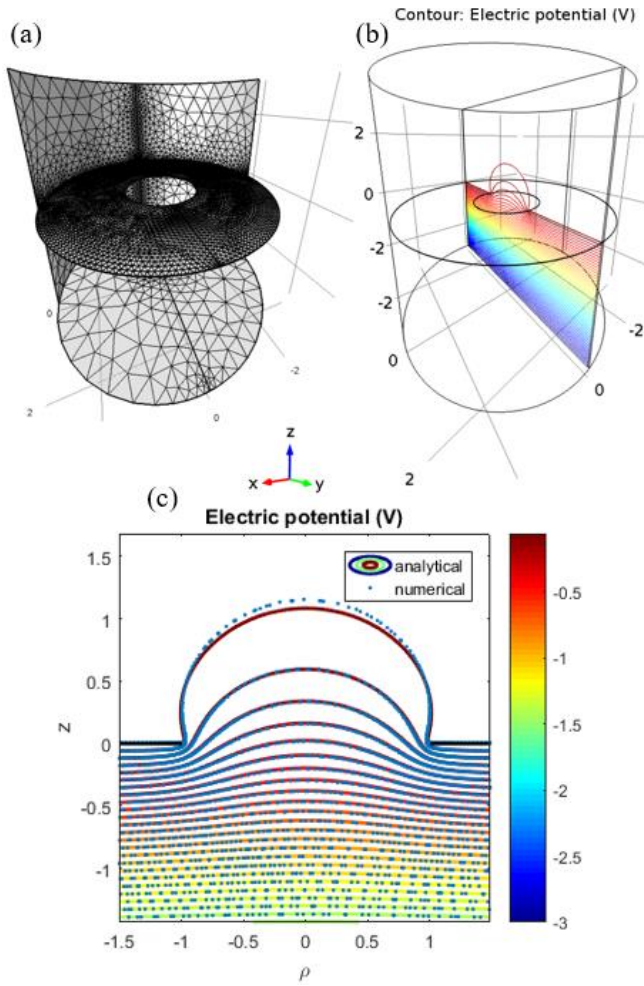


Figure 6. COMSOL finite-element modeling of the electric potential around an iris aperture, a unit module used in both our anode and electrostatic lens. (a) Finite element mesh. (b) Cross-sectional slice of the solution. (c) Cross-sectional slice of the solution validated by the analytical solution.

For pulse durations shorter than 120 ps, temporal profile characterization can be achieved via streaking methods [11], but such methods are laborious and complicated. Instead, we could indirectly infer the temporal duration using the electron energy spread from the measured energy spectrum. Assuming that space charge forces are negligible and the charge density is Gaussian distributed, the rms pulse duration after acceleration by a field E_{acc} can be determined by the electron energy (velocity) spread:

$$\tau_{bunch} = \sqrt{\tau_{uv}^2 + \tau_{spread}^2} \quad (1)$$

$$\text{where } \tau_{spread} = \frac{m\sigma_v}{eE_{acc}}. \quad (2)$$

Here τ_{uv} is the UV laser pulse duration (known), τ_{spread} is the contribution to the temporal spread from the spread in longitudinal velocity σ_v , e is electron charge, and m is electron mass.

5. FUTURE TOFMS INTEGRATION

After the EI source has been characterized, it could be integrated as the front-end EI source on a prototype compact TOFMS system previously developed [12,13] at NASA Goddard Space Flight Center. Sample species will be interrogated and the contribution of our ultrafast e-gun toward enhancement of mass resolution will be measured. We will also experimentally explore the effects of limited detector response time on the system-level performance.

One can predict the ionization yield for a given molecule and a given number of electrons launched into the TOFMS from the EI source. For example, given that we want interrogate methane, which has an ionization cross-section of $\sigma_i = 3.5 \times 10^{-16} \text{ cm}^2$ [14], assuming an interaction length in the gas of $L = 1 \text{ mm}$ and a sample concentration of $n_{gas} = 1 \times 10^{12} \text{ cm}^{-3}$, the EI ionization probability would be 3.5×10^{-5} , as given by

$$\frac{I_{ion}}{I_{e^-}} = \sigma_i L n_{gas}.$$

This corresponds to 1.1×10^4 ions (a typical value for good signal to noise in TOFMS) for every 3.3×10^8 electrons. To achieve this electron yield with our specified laser energy of 5 μJ , the electron gun must have a photoemission efficiency of $> 5 \times 10^{-5}$ photons per electron. To meet this target performance, we plan to either explore the high quantum-efficiency cesium photocathodes discussed in Section 4 or simply increase the available UV energy.

6. CONCLUSION

We have described the design concept of a novel laser-triggered femtosecond EI source which has the potential to improve the mass resolution of TOFMSs. The EI source is based on an ultrafast electron gun triggered by a short pulse UV laser. The ionization source allows TOFMSs to be more compact, extricating the need for bulky multi-bounce flight tubes. Such a TOFMS would enable detailed composition analysis of volatile/atmospheric species on airless bodies, Mars, or ocean worlds (Titan, Enceladus, Europa) and can be deployed on an orbiter or lander. This front-end is not limited to TOFMS instruments; it is applicable to other instrument packages such as ion traps (e.g. LITMS) and Orbitraps (e.g. AROMA). Furthermore, the ultrafast pulsed UV laser technology may be used for other analytical capabilities like laser desorption/ionization on solid samples. Therefore, future development of this system may offer a novel compact instrument package for both atmosphere and surface analysis.

ACKNOWLEDGEMENTS

The authors thank the NASA Goddard Space Flight Center IRAD program for funding this project. The authors also thank Stephanie Getty, Andrej Grubisic, Michael Krainak, and Guangning Yang for valuable discussions.

REFERENCES

- [1] T. T. King et al., "Simulation of a miniature, low-power time-of-flight mass spectrometer for in situ analysis of planetary atmospheres," Proc. SPIE 6959E (2008).
- [2] National Research Council, "Vision and Voyages for Planetary Science in the Decade 2013-2022," p. 11-10 (2011).
- [3] J.J. Zayhowski and A. L. Wilson, "Miniature, pulsed Ti:Sapphire laser system," J. Quantum Elec. 38, 1449 (2002).
- [4] E. Troupaki, M. A. Stephen, A. A. Vasilyev, and A. W. Yu, "Laser Diode Pump Technology for Space Applications," Semiconductor Laser Diode Technology and Applications, 221 (2012).
- [5] C. C. Phifer, "Effects of Radiation on Laser Diodes," Sandia Report SAND2004-4725 (2004). Retrieved from <http://prod.sandia.gov/techlib/access-control.cgi/2004/044725.pdf>
- [6] C. Kolleck et al., "Development of a pulsed UV laser system for laser-desorption mass spectrometry on Mars," ICSO 2010.
- [7] A. Potreck, H. Schröder, M. Lammers, G. Tzeremes, and W. Riede, "Nonlinear optical frequency conversion with KTP and BiBO crystals for lasers in space," Pacific Rim Laser Damage 2014 Opt. Mater. High Power Lasers (2014).
- [8] E. J. Montgomery, D. W. Feldman, P. G. O'Shea, Z. Pan, N. Sennett, K. L. Jensen, and N. A. Moody, "Advances in cesium dispenser photocathodes: modeling and experiment," J. Dir. Energy 3, 66 (2008).
- [9] F. Loehl et al., "High current and high brightness electron sources," Proc. IPAC'10, Kyoto, Japan (2010).
- [10] W. R. Huang, A. Fallahi, X. Wu, H. Cankaya, A-L. Calendron, K. Ravi, D. Zhang, E. A. Nanni, K-H. Hong, F. X. Kärtner, "Terahertz-driven, all-optical electron gun," Optica 3, 11 (2016).
- [11] G. Hairapetian, P. Davis, M. Everett, C. Clayton, C. Joshi, "Streak camera measurements of electron bunch length from a copper photocathode in an RF gun," Proc. PAC'93, Washington DC (1993).
- [12] S. A. Getty, W. B. Brinckerhoff, R. D. Arevalo, M. m> Floyd, X. Li, T. Cornish, S. A. Ecelger, "A Miniature Laser Desorption/Ionization Time-of-Flight Mass Spectrometer for In Situ Analysis of Mars Surface Composition and Identification of Hazards in Advance of Future Manned Exploration," Concept and Approaches for Mars Exploration, Houston, TX (2012).

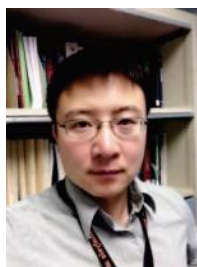
- [13] X. Li, K. Uckert, S. A. Getty, A. Grubisic, W. B. Brinckerhoff, T. Cornish, S. Ecelberger, N. Chanover, "Analysis of aqueous environments by laser desorption/ionization time-of-flight mass spectrometry," IEEE Aerospace Conference (2015).
- [14] Y.-K. Kim, W. Hwang, N. M. Weinberger, M. A. Ali, and M. E. Rudd, "Electron-impact ionization cross sections of atmospheric molecules," J. Chem. Phys. 106, 1026 (1997).

BIOGRAPHY



W. Ronny Huang received a BS in Applied and Engineering Physics from Cornell University in 2009, and a MS and PhD in Electrical Engineering and Computer

Science from MIT in 2017. He was an assistant technical staff at MIT Lincoln Laboratory for 3 years (2009-2012) developing lasers, infrared detectors, and simulation tools. As a PhD student at MIT, he worked on the development of ultrafast THz lasers and electron beams, culminating in a demonstration of the first THz-driven electron gun. He was at NASA Goddard Space Flight Center as a graduate intern for two summers (2016-2017) where he worked on spaceborne lidars and was the PI of the femtosecond ionization time-of-flight mass spectrometer IRAD. He is currently a machine learning researcher at EY New York Innovation Center.



Xiang Li received his B.S. in Chemistry from the Peking University, China in 2003, and Ph.D. in Physical Chemistry from the Johns Hopkins University in 2009. He is an assistant research scientist with a joint appointment at the University of Maryland, Baltimore County and NASA Goddard Space Flight Center.

His research focuses on the detection of trace element and astrobiologically relevant organic molecules in planetary systems, like Mars. He is especially interested in the instrument development of time-of-flight and ion trap mass spectrometers with various ionization and ion gating techniques. He serves as mass spec. scientist for the MOMA ion trap MS on ExoMars and Co-I on development of LITMS and MACROS instrument.

Anthony W. Yu biography not available.



William Brinckerhoff is senior space research associate at NASA's Goddard Space Flight Center. He received his Ph.D. in Physics from the Ohio State University. His current research interests include development of novel miniature mass spectrometers and sample handling systems for planetary missions, synthesis of organic compounds in the interstellar medium, and the habitability of Mars. He serves as a Co-I on MSL/SAM and project scientist for the MOMA ion trap MS on ExoMars.

Molly Fahey biography not available.